Contribution from the Department of Chemistry, University of Michigan, Ann Arbor, Michigan 48109, and Molecular Structure Center, Indiana University, Bloomington, Indiana 47405

Metal-Metal-Bonded Complexes of the Early Transition Metals. 4. Synthesis and Characterization of the Tantalum(III) Dimer $Ta_2Cl_6(PMe_3)_4$[1]

A. P. SATTELBERGER,* R. B. WILSON, JR., and J. C. HUFFMAN

Received October 15, 1981

The dimeric tantalum(III) phosphine complex $Ta_2Cl_6(PMe_3)_4$ (**1**) has been prepared from the reaction of tantalum pentachloride, trimethylphosphine, and sodium amalgam in toluene. The compound crystallizes in the noncentrosymmetric orthorhombic space group $P2_12_12_1$ with $a = 11.681$ (3) Å, $b = 11.834$ (3) Å, $c = 20.257$ (7) Å, $V = 2800.18$ Å^3, and ρ(calcd) = 2.085 g cm^{-3} for mol wt 878.9 and $Z = 4$. The structure refined to $R_F = 0.037$ and $R_{wF} = 0.035$. **1** is a distorted edge-sharing bioctahedral complex with axial phosphines on one tantalum and equatorial phosphines on the second. Direct P-P coupling is observed across the dimer with $J_{PP'} = 2.46$ Hz. The metal-metal bond length in **1** is 2.721 (1) Å, and the formal metal-metal bond order in this d^2-d^2 dimer is 2.

Introduction

Considerable progress has been made in metal-metal multiple-bond chemistry over the past 4 years. The long-standing tungsten-tungsten quadruple bond problem now appears to be solved,[2] new metal-metal multiple bonds have been discovered in group 8 chemistry,[3] and the reactivity of metal-metal bonds is under intense scrutiny.[4] Despite these welcome developments, some enigmas still remain in this area. One of these is the apparent reluctance of niobium and tantalum to form metal-metal-bonded binuclear complexes of the "lower halide" type.[5] Literally hundreds of these are known in molybdenum and tungsten chemistry but relatively few have been reported in group 5 chemistry. Prior to our investigations, the only well-characterized complexes were the $Nb_2Cl_9^{3-}$ salts of Schäfer[6] and the niobium(III) and tantalum(III) halide adducts with tetrahydrothiophene (THT) reported by McCarley and co-workers.[7] The latter are prepared by sodium amalgam reduction of the pentahalides in the presence of excess THT (eq 1). The complexes $Ta_2Cl_6(THT)_3$,[8]

$$MX_5 + 2Na/Hg + THT \xrightarrow{PhCH_3} 0.5M_2X_6(THT)_3 + 2NaX \quad M = Nb, Ta;\ X = Cl, Br \qquad (1)$$

$Ta_2Br_6(THT)_3$,[7] and $Nb_2Br_6(THT)_3$[7] have been studied by X-ray crystallograpy. All adopt the confacial bioctahedral structure found earlier in $Cs_3Nb_2Cl_9$.[6] The diamagnetism and short M-M separations (ca. 2.68-2.73 Å) associated wtih these d^2-d^2 dimers attest the presence of M=M double bonds.

At about the same time we became interested in exploring tantalum dimer chemistry, Sharp and Schrock published their elegant synthetic paper on binuclear tungsten compounds.[2b] Pertinent here was their observation (eq 2, 3) that tungsten

$$(WCl_4)_x + Na/Hg + 2PMe_3 \xrightarrow{THF} 0.5W_2Cl_6(PMe_3)_4 + NaCl \qquad (2)$$

$$W_2Cl_6(PMe_3)_4 + 2Na/Hg \xrightarrow{THF} W_2Cl_4(PMe_3)_4 + 2NaCl \qquad (3)$$

tetrachloride/trimethylphosphine mixtures could be reduced in two discrete steps, first to a binuclear tungsten(III) complex and then to the quadruply bonded tungsten(II) dimer, $W_2Cl_4(PMe_3)_4$. On the basis of these results and the aforementioned observations of McCarley, we made $Ta_2Cl_6(PMe_3)_4$ (**1**) and $Ta_2Cl_4(PMe_3)_4$ (**2**) our synthetic objectives. Our efforts to prepare the triply bonded complex **2** have not been successful to date, but the preparation of **1** is straightforward. Since the latter complex has some interesting chemistry in its own right, we present here the full details of its synthesis and characterization, including our crystallographic results.

Experimental Section

All preparative work was done in a helium-filled Vacuum Atmospheres HE 43-2 drybox. Solvents were purified, dried, and degassed by standard techniques and then stored in the drybox. Tantalum pentachloride was purchased from Pressure Chemical Co. and sublimed before use. Trimethylphosphine was purchased from Orgmet or prepared by the method of Wolfsberger and Schmidbaur.[9] Its purity was checked by proton and ^{31}P NMR.[10] Microanalyses were performed by Galbraith Laboratories, Knoxville, TN.

Preparation of $Ta_2Cl_6(PMe_3)_4$ (1). A toluene solution (50 mL) containing PMe_3 (1.6 g, 21 mmol) was cooled to ca. -20 °C. $TaCl_5$ (3.6 g, 10 mmol) and sodium amalgam (0.5%, 92 g, 20 mmol) were added, and the mixture was warmed to 25 °C and *vigorously* stirred for 2 h. During the reaction, the color of the mixture changed from yellow-orange to green and finally to deep red. The red solution was filtered through Celite, and the reaction vessel was rinsed with an additional 50 mL of toluene. The combined filtrate and washings were reduced in volume to ca. 15 mL. Hexane (20 mL) was then added dropwise with stirring. Filtration gave a microcrystalline burgundy red solid which was washed (2 × 5 mL) with toluene/hexane (1:1) and finally with hexane (5 mL). The yield was ca. 2.6 g.[11] An

* To whom correspondence should be addressed at the University of Michigan.

(1) A preliminary account of this work has appeared: Sattelberger, A. P.; Wilson, R. B., Jr., Huffman, J. C. *J. Am. Chem. Soc.* **1980**, *102*, 7111-7113. For part 3 in this series see: Wilson, R. B., Jr.; Sattelberger, A. P.; Huffman, J. C. *Ibid.* **1982**, *104*, 858-860.

(2) (a) Cotton, F. A.; Fanwick, P. E.; Niswander, R. H.; Sekutowski, J. C. *J. Am. Chem. Soc.* **1978**, *100*, 4725-4732. (b) Sharp, P. R.; Schrock, R. R. *Ibid.* **1980**, *102*, 1430-1431. (c) Sattelberger, A. P.; McLaughlin, K. W.; Huffman, J. C. *Ibid.* **1981**, *103*, 2880-2882.

(3) (a) Cotton, F. A.; Thompson, J. L. *J. Am. Chem. Soc.* **1980**, *102*, 6437-6441. (b) Berry, M.; Garner, C. D.; Hillier, I. H.; MacDowell, A. A. *Inorg. Chim. Acta* **1981**, *53*, L61-L63.

(4) "Reactivity of Metal-Metal Bonds", Chisholm, M. H., Ed.; American Chemical Society: Washington, D. C., 1981; ACS Symp. Ser. No. 155.

(5) Cotton, F. A.; Wilkinson, G. "Advanced Inorganic Chemistry", 4th ed.; Wiley: New York, 1980; Chapter 26.

(6) Broll, A.; Schnering, H. G.; Schäfer, H. *J. Less-Common Met.* **1970**, *22*, 243-245.

(7) Templeton, J. L.; Dorman, W. C.; Clardy, J. C.; McCarley, R. E. *Inorg. Chem.* **1978**, *17*, 1263-1267 and references therein.

(8) Cotton, F. A.; Najjar, R. C. *Inorg. Chem.* **1981**, *20*, 2716-2719. This paper also described the synthesis and X-ray structure of $Ta_2Cl_6[S(CH_3)_2]_3$. The structures of the THT and dimethyl sulfide complexes are virtually identical.

(9) Wolfsberger, W.; Schmidbaur, H. *Synth. React. Inorg. Met.-Org. Chem.* **1974**, *4*, 149-156.

(10) ^1H NMR (ppm, C_6D_6, 360 MHz): 0.79 ($J_{PH} = 2.75$ Hz). ^{31}P NMR (ppm, C_6D_6, 145.8 MHz, $\{^1H\}$): -63.3 (s). All of the NMR data reported in this paper were recorded on a Bruker 360. Proton and ^{31}P NMR spectra were recorded at 360.1 and 145.8 MHz, respectively. Proton chemical shifts in ppm from $(CH_3)_4Si$. ^{31}P chemical shifts are in ppm from external H_3PO_4; shifts are negative for lines upfield of H_3PO_4.

(11) This reaction has been successfully scaled up by a factor of four. We recommend the use of an overhead mechanical stirrer and a Morton flask for large scale preparations.

0020-1669/82/1321-2392$01.25/0

Table I. Crystal Data for $Ta_2Cl_6(PMe_3)_4$

mol formula	$Ta_2Cl_6P_4C_{12}H_{36}$	min abs	0.261
color	burgundy red	max abs	0.394
cryst dimens, mm	0.06 × 0.10 × 0.13	2θ range, deg	5-50
space group	$P2_12_12_1$	no. of data with $F_o > 2.33\sigma(F_o)$	2610
cell dimens[a]			
a, Å	11.681 (3)	final residuals	
b, Å	11.834 (3)	R_F	0.037
c, Å	20.257 (7)	R_{wF}	0.035
molecules/cell	4	goodness-of-fit, last cycle	1.015
cell *V*, Å^3	2800.18	max Δ/σ, last cycle	0.05
d(calcd), g cm^{-3}	2.085		
λ, Å	0.710 69		
mol wt	878.9		
linear abs coeff	85.2		

[a] At −170 °C; 42 reflections.

analytically pure sample was obtained by recrystallization from concentrated toluene solution at −40 °C.[12]

Anal. Calcd for $Ta_2Cl_6(PMe_3)_4$ ($Ta_2Cl_6P_4C_{12}H_{36}$): C, 16.40; H, 4.13; Cl, 24.20. Found: C, 16.53; H, 4.12; Cl, 24.42. Molecular weight for $Ta_2Cl_6(PMe_3)_4$: calcd, 879; found, 876.

^1H NMR (ppm, C_6D_6, 360 MHz): 1.23 (virtual triplet, 1, axial PMe_3, J_{PH} (apparent) = 3.97 Hz), 1.11 (d, 1, equatorial PMe_3, J_{PH} = 7.93 Hz).

$^{31}P\{^1H\}$ NMR (ppm, C_6D_6, 145.8 MHz): −31.1 (t, 1, equatorial PMe_3, $J_{PP'}$ = 2.46 Hz), −52.3 (t, 1, axial PMe_3, $J_{PP'}$ = 2.46 Hz).[13]

X-ray Crystallography. Suitable crystals of **1** were grown from concentrated toluene solutions, carefully layered with methylcyclohexane at −40 °C. A single crystal was mounted on a glass fiber with Dow Corning silicon grease in a nitrogen-filled drybag and transferred to the liquid-nitrogen boil-off cooling system of the diffractometer. Diffraction data were collected at −170 ± 4 °C by a θ–2θ scan technique with equipment described in detail elsewhere.[14] The analytical form of the scattering factors[15a] for neutral tantalum, chlorine, phosphorus, carbon, and hydrogen was corrected for both the real and imaginary components of anomolous dispersion.[15b] Data were corrected for absorption and the structure solved by a combination of Patterson, difference Fourier, and full-matrix least-squares refinement techniques. All nonhydrogen atoms were located and their positional and thermal parameters (anisotropic for Ta, Cl, P, and C) refined. A test for crystal chirality was made at this point by transforming all atomic coordinates from (x, y, z) to $(-x, -y, -z)$. Further refinement resulted in a significant decrease in the residuals, R_F and R_{wF}, indicating that our original choice of chirality was incorrect. All of the methyl protons were located by difference Fourier techniques in the correct enantiomorph, and their positional and thermal parameters were varied in the final stages of refinement. Final residuals and other pertinent crystallographic parameters are listed in Table I. Final atomic coordinates and isotropic thermal parameters are given in Table II.[16]

Results and Discussion

Synthesis and Physiochemical Properties of $Ta_2Cl_6(PMe_3)_4$ (1). The synthetic approach (eq 4) employed to prepare the

$$TaCl_5 + 2Na/Hg + 2PMe_3 \xrightarrow{PhCH_3} 0.5Ta_2Cl_6(PMe_3)_4 + 2NaCl \quad (4)$$

title compound was simple and direct. A series of color changes were noted during the course of the reaction. Tantalum(IV) compounds, e.g., $TaCl_4(PMe_3)_2$,[17] are likely intermediates, but no attempt has been made to isolate them. **1** is a burgundy red solid and has been isolated in yields of up to 75%. The workup described in the Experimental Section gives slightly lower yields (~60%) but is more reliable than our orginal procedure and gives a product which is pure by ^1H NMR. The complex is sensitive to oxygen and water, decomposing within minutes in laboratory air. Attempts to obtain the mass spectrum of **1** were unsuccessful.

$Ta_2Cl_6(PMe_3)_4$ is soluble in aromatic and ether solvents, insoluble in hexane, and decomposes in chloroform and methylene chloride. The proton NMR spectrum of **1** (in C_6D_6) is shown in Figure 1. There are two methyl resonances (each of area one); the virtual triplet at δ 1.23 is assigned to a pair of axial phosphine ligands and the "doublet" at δ 1.11 to a pair of equatorial phosphine ligands (vide infra). In the $^{31}P\{H\}$ NMR spectrum two resonances are also observed at δ −31.1 and −52.3, again in a 1:1 ratio. These resonances are actually closely spaced 1:2:1 triplets (i.e., an A_2X_2 spin system) with $J_{PP'}$ = ±2.46 Hz. The observation of P–P coupling across a

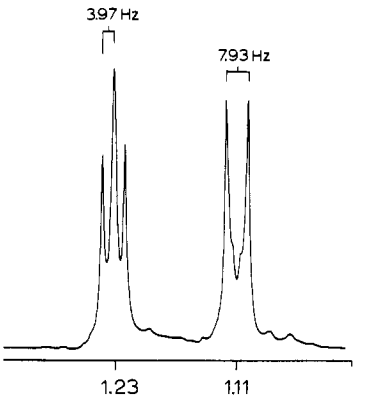

Figure 1. 360-MHz proton NMR spectrum of **1** (C_6D_6 solution) showing the two phosphine methyl resonances. Chemical shifts (δ) are in ppm from Me_4Si.

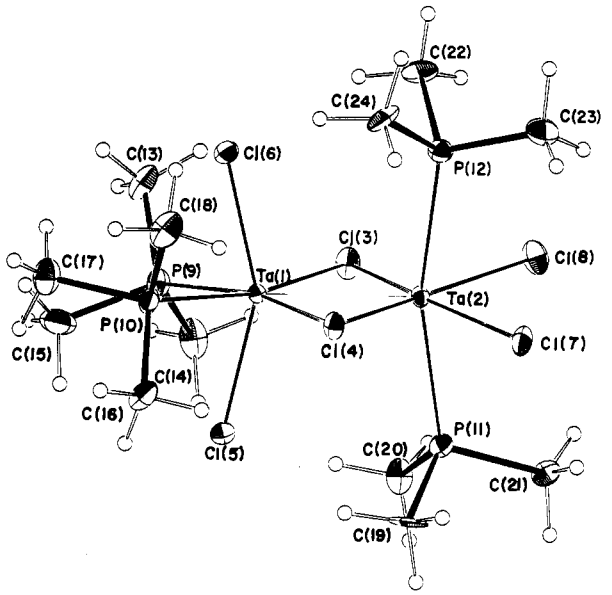

Figure 2. ORTEP drawing of **1** showing the atom numbering scheme used in Tables II–V.

(12) Reactions with other phosphines (e.g., PEt_3, PBu_3, $PMePh_2$) have not provided tractable products. See also: Cotton, F. A.; Najjar, R. C. *Inorg. Chem.* **1981**, *20*, 1866–1869.

(13) The ^{31}P NMR splittings reported here were not resolved at 36.2 MHz[1] and were resolved at 145.8 MHz only after a considerable effort was made to maximize the shimming. We note that the splittings (2.46 Hz) are comparable to the line widths at half-height (ca. 2 Hz) in this complex. The ^{31}P chemical shifts reported here are the *correct* ones and supercede those reported earlier.[1]

(14) Huffman, J. C.; Lewis, L. N.; Caulton, K. G. *Inorg. Chem.* **1980**, *19*, 2755–2762.

(15) "International Tables for X-ray Crystallography"; Kynoch Press: Birmingham, England, 1974; Vol. 4: (a) pp 99–101; (b) pp 149–150.

(16) A table of anisotropic thermal parameters is provided as supplementary material.

(17) Sodium amalgam reductions of $TaCl_5$ in the presence of 1,2-bis(dimethylphosphino)ethane (dmpe) provide monomeric $TaCl_4(dmpe)_2$ when 1 equiv of reducing agent is used in benzene/THF mixtures. See: Datta, S.; Wreford, S. S. *Inorg. Chem.* **1977**, *16*, 1134–1137. The complexes $NbCl_4(PMe_3)_2$ and $NbCl_4(PEt_3)_2$ are also known. See: Manzer, L. E. *Inorg. Chem.* **1977**, *16*, 525–528.

Table II. Fractional Coordinates for $Ta_2Cl_6[P(CH_3)_3]_4$[a,b]

atom	10^4x	10^4y	10^4z	$10B_{iso}$, Å^2
Ta(1)	5767.7 (4)	807.4 (4)	8735.5 (2)	8
Ta(2)	7690.6 (4)	−443.6 (4)	8534.0 (2)	9
Cl(3)	7613 (3)	1118 (3)	9310 (2)	15
Cl(4)	5896 (2)	−800 (3)	7962 (1)	13
Cl(5)	5831 (3)	2173 (3)	7862 (2)	17
Cl(6)	4969 (3)	−14 (3)	9716 (2)	14
Cl(7)	8316 (3)	−1910 (3)	7743 (2)	16
Cl(8)	9616 (3)	−632 (3)	9046 (2)	20
P(9)	5442 (3)	2738 (3)	9387 (2)	14
P(10)	3640 (3)	451 (3)	8335 (2)	14
P(11)	8618 (3)	834 (3)	7638 (2)	14
P(12)	7187 (3)	−2113 (3)	9330 (2)	14
C(13)	5308 (12)	2608 (13)	10271 (7)	21
C(14)	6623 (13)	3743 (12)	9301 (8)	22
C(15)	4232 (15)	3607 (13)	9163 (7)	27
C(16)	3407 (11)	542 (15)	7458 (6)	21
C(17)	2535 (12)	1313 (12)	8706 (8)	22
C(18)	3121 (11)	−947 (12)	8516 (8)	22
C(19)	7885 (13)	840 (14)	6851 (7)	24
C(20)	8862 (12)	2301 (12)	7826 (7)	18
C(21)	10038 (12)	377 (13)	7393 (7)	20
C(22)	7277 (15)	−1731 (14)	10196 (7)	29
C(23)	8162 (13)	−3287 (13)	9256 (8)	27
C(24)	5788 (13)	−2810 (12)	9269 (7)	22
atom	10^3x	10^3y	10^3z	B_{iso}, Å^2
H(25)	483 (10)	236 (10)	1042 (6)	0 (3)
H(26)	591 (10)	198 (10)	1066 (6)	1 (3)
H(27)	547 (12)	332 (13)	1058 (8)	3 (3)
H(28)	731 (12)	340 (11)	962 (7)	5 (3)
H(29)	658 (15)	393 (17)	891 (9)	4 (7)
H(30)	652 (9)	422 (10)	960 (6)	0 (2)
H(31)	430 (10)	373 (10)	883 (6)	0 (3)
H(32)	336 (10)	335 (10)	928 (6)	0 (2)
H(33)	436 (10)	451 (10)	948 (6)	2 (2)
H(34)	349 (10)	113 (10)	733 (6)	0 (5)
H(35)	407 (15)	7 (14)	713 (8)	8 (4)
H(36)	257 (11)	55 (10)	734 (6)	1 (3)
H(37)	253 (11)	174 (10)	847 (6)	0 (4)
H(38)	200 (14)	105 (13)	864 (8)	3 (4)
H(39)	242 (10)	148 (9)	916 (6)	0 (2)
H(40)	236 (12)	−87 (11)	852 (6)	1 (3)
H(41)	377 (36)	−116 (37)	841 (23)	31 (18)
H(42)	311 (10)	−97 (10)	890 (6)	0 (3)
H(43)	819 (11)	127 (11)	654 (7)	1 (4)
H(44)	789 (10)	9 (10)	676 (6)	0 (2)
H(45)	714 (15)	93 (14)	700 (8)	6 (4)
H(46)	938 (10)	289 (10)	737 (6)	2 (2)
H(47)	833 (12)	256 (12)	806 (7)	1 (4)
H(48)	923 (11)	255 (10)	827 (6)	2 (2)
H(49)	998 (9)	−20 (10)	722 (5)	0 (2)
H(50)	1041 (10)	81 (10)	718 (6)	0 (2)
H(51)	1058 (14)	52 (14)	776 (8)	4 (4)
H(52)	793 (11)	−154 (10)	1025 (6)	0 (3)
H(53)	687 (12)	−97 (13)	1033 (7)	2 (4)
H(54)	724 (13)	−232 (13)	1053 (8)	3 (3)
H(55)	794 (11)	−364 (11)	860 (7)	7 (3)
H(56)	877 (11)	−290 (11)	922 (6)	1 (3)
H(57)	804 (10)	−370 (11)	944 (6)	0 (3)
H(58)	494 (10)	−242 (10)	937 (6)	1 (3)
H(59)	590 (10)	−298 (9)	885 (6)	0 (2)
H(60)	580 (10)	−325 (10)	955 (6)	0 (6)

[a] The isotropic thermal parameters listed for those atoms refined anisotropically are the isotropic equivalent from the formula given by: Hamilton, W. C. *Acta Crystallogr.* **1959**, *12*, 609. [b] Numbers in parentheses in this and all following tables refer to the error in the least significant digits.

metal–metal-bonded dimer is rare but has been reported previously.[18] The question of which ^{31}P resonance to assign to the axial phosphines and which to assign to the equatorial phosphines was resolved by selective ^1H decoupling experiments. Irradiation of the ^1H virtual triplet at δ 1.23 with low-power RF noise left the δ −52.3 ^{31}P signal virtually unchanged while the δ −31.1 resonance broadened significantly due to P–H coupling. A similar experiment with ^1H irradiation at δ 1.11 had the opposite effect. Therefore, we assign the ^{31}P δ −31.1 signal to the equatorial phosphines and the δ −52.3 resonance to the axial phosphines.

(18) Girolami, G. S.; Mainz, V. V.; Anderson, R. A.; Vollmer, S. H.; Day, V. W. *J. Am. Chem. Soc.* **1981**, *103*, 3953–3955.

Table III. Selected Bond Distances (Å) in 1

A	B	dist	A	B	dist
Ta(1)	Ta(2)	2.721 (1)	P(9)	C(13)	1.804 (16)
Ta(1)	Cl(3)	2.477 (3)	P(9)	C(14)	1.830 (16)
Ta(1)	Cl(4)	2.470 (3)	P(9)	C(15)	1.805 (18)
Ta(1)	Cl(5)	2.398 (3)	P(10)	C(16)	1.802 (14)
Ta(1)	Cl(6)	2.400 (3)	P(10)	C(17)	1.808 (16)
Ta(1)	P(9)	2.666 (4)	P(10)	C(18)	1.801 (17)
Ta(1)	P(10)	2.647 (3)	P(11)	C(19)	1.810 (15)
Ta(2)	Cl(3)	2.427 (3)	P(11)	C(20)	1.800 (14)
Ta(2)	Cl(4)	2.433 (3)	P(11)	C(21)	1.813 (15)
Ta(2)	Cl(7)	2.472 (3)	P(12)	C(22)	1.815 (15)
Ta(2)	Cl(8)	2.487 (3)	P(12)	C(23)	1.803 (18)
Ta(2)	P(11)	2.598 (4)	P(12)	C(24)	1.835 (16)
Ta(2)	P(12)	2.617 (3)			

Table IV. Selected Bond Angles (Deg) in 1

A	B	C	angle
Ta(2)	Ta(1)	Cl(3)	55.4 (1)
Ta(2)	Ta(1)	Cl(4)	55.7 (1)
Ta(2)	Ta(1)	Cl(5)	103.3 (1)
Ta(2)	Ta(1)	Cl(6)	103.0 (1)
Ta(2)	Ta(1)	P(9)	131.2 (1)
Ta(2)	Ta(1)	P(10)	130.0 (1)
Cl(3)	Ta(1)	Cl(4)	111.1 (1)
Cl(5)	Ta(1)	Cl(6)	153.6 (1)
Cl(5)	Ta(1)	P(9)	78.0 (1)
Cl(5)	Ta(1)	P(10)	84.8 (1)
Cl(6)	Ta(1)	P(9)	83.2 (1)
Cl(6)	Ta(1)	P(10)	79.9 (1)
P(9)	Ta(1)	P(10)	98.9 (1)
Ta(1)	Ta(2)	Cl(3)	57.2 (1)
Ta(1)	Ta(2)	Cl(4)	56.9 (1)
Ta(1)	Ta(2)	Cl(7)	136.3 (1)
Ta(1)	Ta(2)	Cl(8)	137.1 (1)
Ta(1)	Ta(2)	P(11)	97.6 (1)
Ta(1)	Ta(2)	P(12)	97.6 (1)
Cl(3)	Ta(2)	Cl(4)	114.1 (1)
Cl(7)	Ta(2)	Cl(8)	86.6 (1)
Cl(7)	Ta(2)	P(11)	80.3 (1)
Cl(7)	Ta(2)	P(12)	86.3 (1)
Cl(8)	Ta(2)	P(11)	88.1 (1)
Cl(8)	Ta(2)	P(12)	83.0 (1)
P(11)	Ta(2)	P(12)	164.4 (1)
Ta(1)	Cl(3)	Ta(2)	67.4 (1)
Ta(1)	Cl(4)	Ta(2)	67.4 (1)
Ta(1)	P(9)	C(13)	115.5 (6)
Ta(1)	P(9)	C(14)	113.7 (5)
Ta(1)	P(9)	C(15)	118.4 (6)
C(13)	P(9)	C(14)	102.4 (8)
C(13)	P(9)	C(15)	103.3 (7)
C(14)	P(9)	C(15)	101.3 (8)

Solid-State Structure. In the crystalline state the compound is composed of discrete molecules of $Ta_2Cl_6(PMe_3)_4$. An ORTEP view of the molecule indicating the coordination geometry and the atom-numbering scheme is shown in Figure 2. A second ORTEP drawing showing a blowup of the inner core of the dimer is presented in Figure 3. Selected bond distances and angles are given in Tables III and IV, respectively.

The molecule consists of two somewhat distorted octahedra sharing a common edge. The extent of these distortions can be understood by examination of Figure 3 and by consideration of the angles between least-squares planes of the dimers inner core. The metal–metal separation of 2.721 (1) Å and the acute Ta–Cl_b–Ta angles (θ_b = 67.4(1)°) are taken as indications of

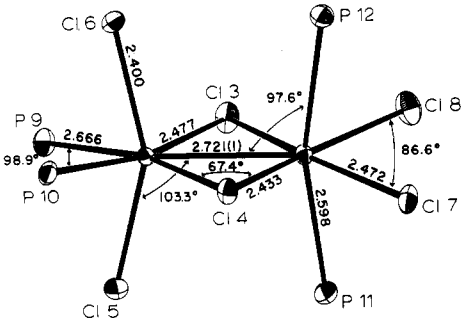

Figure 3. ORTEP drawing of the inner core of **1**. Error estimates on bond distances and angles are given in Tables III and IV, respectively.

strong metal–metal bonding (vide infra), and this bonding interaction has a pronounced effect on the solid-state conformation of the dimer. The rhombiod of tantalum atoms and bridging chlorines is planar, but this plane does not include the equatorial ligands (Cl(7) and Cl(8) are displaced ±0.27 Å, respectively, and the phosphorus atoms, P(9) and P(10), are displaced ±0.37 Å, respectively). These deviations from basal planarity are, almost certainly, the result of nonbonded interactions between axial substituents. Partial relief from H···Cl contacts is provided by a bending back of the axial ligands (see Figure 3), but the extent to which this bending can occur is limited by the steric requirements of the equatorial ligands. If bending alone cannot relieve the axial steric interactions, then the only option is to twist the end groups away from each other, as observed.

The foregoing analysis provides a reasonable explanation for the distortions in **1** but it sidesteps a more fundamental question—why does **1** adopt a structure with equatorial and axial phosphines? If steric factors were the only consideration, then **1** should have all of the bulky phosphine ligands in equatorial sites where crowding is less severe. The fact that **1** adopts the more congested configuration implies a delicate balance between steric and electronic effects with the latter dictating the ultimate stereochemistry. We believe that the alternation in equatorial and axial tantalum–ligand bond lengths in **1** (Table III and Figure 3) are a manifestation of these electronic effects, but we need to examine other derivatives before any significant conclusions can be reached.[19]

Metal–Metal Bonding in $Ta_2Cl_6(PMe_3)_4$. The assignment of metal–metal bond orders in bridged binuclear complexes is a sensitive issue and one which has been discussed by several authors.[20] In the case of **1** the experimental *facts* are these: (1) The tantalum atoms are separated by only 2.721 (1) Å, a distance which is ~0.24 Å shorter than that found in $[Ta_6Cl_{12}]Cl_2 \cdot 7H_2O$[21] and comparable to those found in $Ta_2Cl_6(THT)_3$[8] and $Ta_2Br_6(THT)_3$.[7] In edge-sharing bioctahedral $[TaCl(NMe_2)_2]_2(\mu\text{-}Cl)_2$,[22] a complex with no metal–metal bond, the Ta–Ta separation is ca. 4.1 Å. (2) Ta–Cl_b–Ta angle (θ_b) is compressed to 67.4 (1)° from the ideal edge-sharing bioctahedral value of 90.0°. (3) There are distortions in the dimers core (e.g., bending back of the axial ligands and twisting of the axial ligands away from each other) which could be relieved by lengthening the metal–metal bond and opening θ_b. Together, these facts lead to the logical conclusion that there is a metal–metal bond in **1**, but there remains the question of bond order. We are guided here by the extended Hückel molecular orbital calculations of Shaik, Hoffmann, Fisel, and Summerville[23] (SHFS) on bridged M_2L_{10} complexes. We will review briefly some of their observations and then show how they apply to **1** and a related complex which were not considered by SHFS. The arguments which follow will focus on the $M_2(\mu\text{-}Cl)_2$ core of the D_{2h} M_2Cl_{10} dimer. Of course, by using M_2Cl_{10} as a model compound, we ignore the unusual phosphine stereochemistry in **1** but our objective here is to understand the metal–metal bonding in **1** and not the relative energies of $M_2Cl_6L_4$ dimer configurations.

The six low-lying d-orbitals that characterize the inner rhomboid of bioctahedral M_2Cl_{10} are shown schematically in

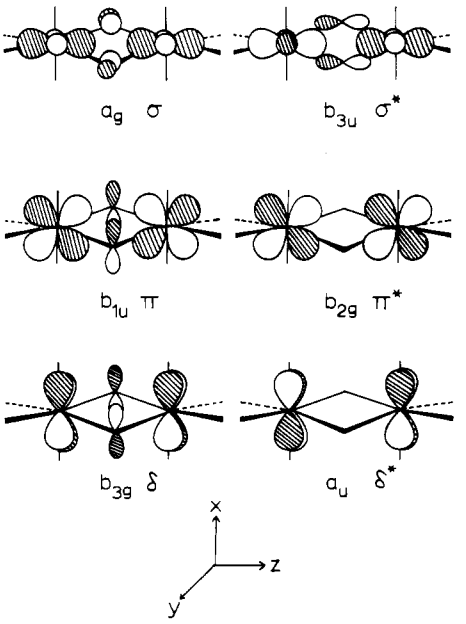

Figure 4. Six lower d-block orbitals of an edge-sharing bioctahedral M_2L_{10} complex.

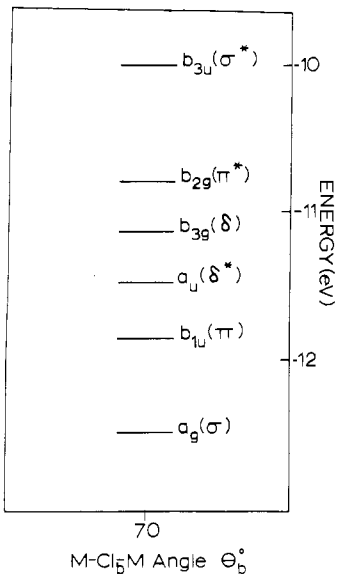

Figure 5. Energies of the Re_2Cl_{10} d-block orbitals at $\theta_b = 70°$. The π level is the highest filled MO in **1**. See text.

(19) *One* way to explain the shortening of axial bond lengths would be to invoke Cl pπ → M dδ^* *and* M dπ → P dπ back-bonding (see Figures 4 and 5). In principle, this hypothesis can be tested by synthesizing a whole series of compounds: $Ta_2X_6L_4$, where X = Cl, Br and L = PMe_3, $P(OMe)_3$, and NMe_3. Efforts to prepare some of these derivatives are under way in our laboratory.

(20) (a) Cotton, F. A. *Rev. Pure Appl. Chem.* **1967**, *17*, 25–40. (b) Dahl, L. F.; Rodulfo, de Gil, E.; Feltham, R. D. *J. Am. Chem. Soc.* **1969**, *91*, 1653–1664. (c) Summerville, R. H.; Hoffmann, R. *Ibid.* **1976**, *98*, 7240–7254.

(21) Burbank, R. D. *Inorg. Chem.* **1966**, *5*, 1491–1498. The metal–metal bond order in the $Ta_6Cl_{12}^{2+}$ cation is $^2/_3$. See: Cotton, F. A.; Haas, T. E. *Ibid.* **1964**, *3*, 10–17.

(22) Chisholm, M. H.; Huffman, J. C. Tan, L. *Inorg. Chem.* **1981**, *20*, 1859–1866.

(23) Shaik, S.; Hoffmann, R.; Fisel, C. R.; Summerville, R. H. *J. Am. Chem. Soc.* **1980**, *102*, 4555–4572.

Figure 4. The orbitals are labeled according to D_{2h} symmetry and by their cylindrical pseudosymmetry. They are the bonding and antibonding combinations of metal d functions whose ancestors are the octahedral t_{2g} orbitals. The symmetry allowed mixing-in of bridging chlorine p orbitals is also shown in the figure. In Figure 5, we reproduce that portion of the SHFS Re_2Cl_{10} energy level diagram (their Figure 2) where $\theta_b = 70°$. The ordering of dimer valence MOs is $\sigma < \pi < \delta^* < \delta < \pi^* < \sigma^*$. The four available 5d electrons in **1** would fill the σ and π levels giving a formal metal–metal bond order of 2.[24]

There is another early-transition-metal dimer whose structural characterization has revealed an overall geometry and ligand stereochemsitry similar to that observed in **1**. This complex, $W_2Cl_6(py)_4$ (**3**)[25] is a d^3–d^3 system. According to the SHFS–MO diagram, the additional electrons in **3** (relative to **1**) will fill the δ^* orbital, giving the ground-state electronic configuration $\sigma^2\pi^2\delta^{*2}$ and a formal metal-metal bond order of 1. The slight increase in M–M separation (2.721 (1) → 2.737 (3) Å) and θ_b (67.4 (1)° → 69.8 (2)°) going from **1** to **3**, coupled with the absence of basal distortions in **3**, are consistent with this prediction and our prejudice that π bonding should be worth considerably more than δ antibonding. These simple ideas will be tested as more X-ray structural data on $M_2Cl_6L_4$ complexes become available.[26]

Before leaving this section, we should point out that SHFS actually predict that $M_2D_8(\mu\text{-}D)_2$ complexes where D is a donor ligand (e.g., chlorine, phosphide, phosphine, etc.) should have θ_b values closer to 100° and nonbonded M–M separations for any d-electron count from d^1–d^1 to d^5–d^5. This prediction was made after a careful analysis of core effects, the most important of which appears to be the repulsive interaction between axial substituents. The d^2–d^2 dimer, Re_2Cl_{10}, fits nicely into this picture. The Re–Re separation, at 3.74 Å, is certainly a nonbonded one, and the value of θ_b is 98.1°, in excellent agreement with the calculated optimal value of 102.5°. Why are the $M_2(\mu\text{-}Cl)_2$ cores in Re_2Cl_{10} and $Ta_2Cl_6(PMe_3)_4$ so different? We would argue that the high positive charge on rhenium causes contraction of the valence atomic orbitals to the extent that overlap between metal orbitals is too small at any reasonable value of θ_b (say down to 65°) to allow effective bond formation and that, as predicted, the molecule moves along the M_2Cl_{10} potential energy surface to $\theta_b = 98.1°$, where axial interactions can be minimized. In the case of **1**, the formal oxidation state is 3+ and the positive charge on tantalum will be tempered by the presence of the phosphine ligands which are good σ donors. As such, we expect a much better overlap of metal orbitals at low values ($\sim$70°) of θ_b and the stabilization afforded by M–M bond formation. In view of the distortions involving axial substituents in **1**, this stabilization must be quite substantial.

Conclusions

The chemistry of tantalum has, thus far, been dominated by the 5+ oxidation state. We, and others,[22] are inclinded to believe that tantalum in its lower oxidation states can enter into interesting homodinuclear relationships. The isolation of **1**, its structural characterization, and its reactivity toward molecular hydrogen[1] are certainly advertisements for this point of view. Future reports in this series will focus on the reaction chemistry of **1** and our efforts to develop tantalum(II) and tantalum(IV) binuclear chemistry.

Acknowledgment. The authors thank Professor Roald Hoffmann and R. E. McCarley for their comments on bridged M_2L_{10} complexes. The Research Corp., the donors of the Petroleum Research Fund, administered by the American Chemical Society, and the U.S. Department of Energy (Grant No. DE-FG02-80ER10125) are acknowledged for support of this work. We also thank the Marshall H. Wrubel Computing Center, Indiana University, for a generous gift of computer time. The Bruker 360 NMR spectrometer was purchased, in part, by funds provided by the National Science Foundation.

Registry No. **1**, 75592-89-1; $TaCl_5$, 7721-01-9.

Supplementary Material Available: Tables of observed and calculated structure factors, anisotropic thermal parameters, and angles between least-squares planes (20 pages). Ordering information is given on any current masthead page. The complete structure report, MSC 8099, is available in microfiche form only from the Indiana University Chemistry Library.

(24) It is important to point out that the basic features of the SHFS–MO diagram have been verified in more sophisticated calculations of the Fenske–Hall type. See: Anderson, L. B.; Cotton, F. A.; DeMarco, D.; Fang, A.; Ilsley, W. H.; Kolthammer, B. W. S.; Walton, R. A. *J. Am. Chem. Soc.* **1981**, *103*, 5078–5086.

(25) Jackson, R. B.; Streib, W. E. *Inorg. Chem.* **1971**, *10*, 1760–1763.

(26) The syntheses of $W_2Cl_6(THF)_4$ and $W_2Cl_6(PMe_3)_4$ have been reported.[2b] From NMR spectral measurements, it appears that both have structures similar to **1** and **3** but no X-ray data are available at this time.